ISSN 1990-7931, Russian Journal of Physical Chemistry B, 2010, Vol. 4, No. 1, pp. 101–109. © Pleiades Publishing, Ltd., 2010.
Original Russian Text © V.Ya. Basevich, B.V. Lidskii, S.M. Frolov, 2010, published in Khimicheskaya Fizika, 2010, Vol. 29, No. 2, pp. 38–47.

COMBUSTION, EXPLOSION, AND SHOCK WAVES

Mechanisms of the Amplification of a Shock Wave Passing through a Cool Flame Zone

V. Ya. Basevich, B. V. Lidskii, and S. M. Frolov

Semenov Institute of Chemical Physics, Russian Academy of Sciences, Moscow, 119991 Russia

e-mail: Smfrol@chph.ras.ru

Received December 9, 2008

Abstract—A theoretical explanation of the Shchelkin–Sokolik effect, that is the dependence of the predetonation distance on the duration of thermal pretreatment of the explosive mixture before its ignition with an external source, is presented. Gasdynamic and kinetic calculations of the direct initiation of detonation in an *n*-pentane–oxygen mixture based on a simplified and a detailed kinetic mechanism are performed. It is demonstrated that a thermal pretreatment of the mixture causes a shortening of the predetonation distance, with the shortest predetonation distance being achieved when the shock wave arrives at the moment the cool flame arises. The calculated and measured dependences of the predetonation distance on the duration of thermal pretreatment of the mixture are demonstrated to be satisfactory agreement. The role played by the wall reactions is discussed.

DOI: 10.1134/S1990793110010161

1. INTRODUCTION

At present, the possibility of using the controlled detonation explosion of explosive gas and spray mixtures in aircraft propulsion systems and in powerful pulse burners is being intensely explored [1, 2]. One of the key problems in the way to practical applications of detonation explosion is to ensure a reliable deflagration-to-detonation transition (DDT) at a low energies of ignition of the mixture (up to 1 J) in relatively short tubes (up to 2–3 m in length). There are a number of physical and chemical methods for solving this problem, at least partially. The physical methods include a decrease in the tube diameter [3], installation in the tube of a wire spiral [4] or turbulizing obstacles of special shape [5], installation of several flashboxes in the tube [6], bending of the tube to form a coil or two U-shaped turns [7], use of nanosecond pulsed discharges [8, 9], etc. The chemical methods encompass the known means of enhancing the sensitivity of the explosive mixture by various pretreatments (before ignition), such as thermal treatment [10], introduction of chemically active additives [11], rapid mixing with hot combustion products [12], partial decomposition of the fuel to form more active intermediate products [13], treatment of the oxidizer with a electric discharge or laser radiation to produce excited molecules [14], etc. A extensive review of relevant studies can be found in [15].

The aim of the present work was to try to quantitatively describe the dependence of the predetonation distance on the duration of thermal pretreatment of the explosive mixture before its ignition by an external source, known as the Shchelkin–Sokolik effect [10]. The authors of [10] demonstrated that a thermal pretreatment of the combustible mixture before spark ignition could shorten the DDT distance nearly twofold. Given that this work was published more than 70 years ago, we would like to epitomize its content.

2. SHCHELKIN–SOKOLIK EFFECT

The experiments in [10] were performed in a closed glass tube, 110 cm in length and 20 mm in inner diameter, which was placed into an electric oven, which had a slit for photorecording of flame propagation and DDT on a moving film. At one of the tube ends, a spark plug was installed. The test explosive mixture was a homogeneous mixture of petroleum ether (a fraction boiling at 38–40°C, which in [10] was conventionally referred to as pentane) with oxygen at a fuel equivalence ratio of $\Phi \approx 1.1$. The mixture was prepared manometrically and kept in a reservoir, from which it was admitted into the reaction tube heated to $T_0 = 325$–400°C (here and below, the subscript 0 denotes the initial state). The time it took for the mixture to flow over from the reservoir into the tube was 0.4–0.6 s. The pressure and temperature were selected so as to make the mixture undergo cool-flame oxidation without autoignition. This was accomplished by decreasing the pressure to $p_0 = 0.33$–0.49 atm. In preliminary experiments (without spark ignition), the induction period τ of the cool flame was measured as the time elapsed from the end of mixture flow-over to the emergence of a pressure spike, which was recorded with a sensitive membrane manometer. The emergence of the cool flame was accompanied by a temperature rise of 200 to 300°C and a weak luminescence of the gas. Depending on the temperature and pressure of the mixture in the tube, the induction period of development of the cool flame range within 0.4–3.6 s. In

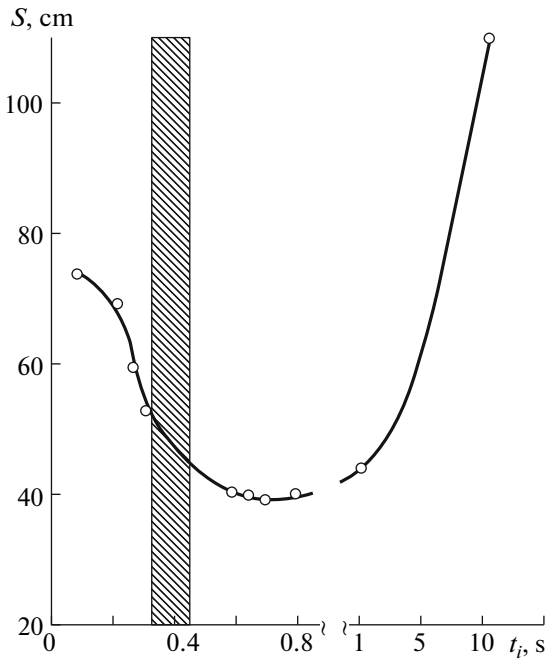

Fig. 1. Dependence of the predetonation distance S on the spark ignition delay t_i [10]; C_5H_{12} : $8O_2$ mixture; initial temperature, $T_0 = 608$ K; initial pressure $p_0 = 0.42$ atm. The hatched band indicates the uncertainty in the cool flame induction period.

the main series of experiments with spark ignition of the mixture, three parameters were varied: the spark ignition delay t_i (the time interval from the end of mixture flow-over to the moment the mixture was ignited by spark) and the initial temperature T_0 and pressure p_0 of the mixture. After the mixture was ignited near the closed end of the tube, an accelerated propagation of the flame was first observed. Detonation arose in the region between the shock wave and the flame front; it was identified by the appearance of a new highly luminous front with a different slope in photographic records and by the formation of a retonation wave propagating in the opposite direction. The predetonation distance S was determined from photographic records as the distance from the spark plug to the location where the luminous front slope changed drastically.

The results of an experiment from [10] at $T_0 =$ 335°C and $p_0 = 0.42$ atm are displayed in Fig. 1 as the dependence of the predetonation distance on the spark ignition delay t_i. Because of uncertainties in measuring τ, the moment of emergence of the cool flame is indicated with a 0.2-s-wide hatched band. The main result of the experiments described in [10] is "that the predetonation distance significantly decreases if the mixture is ignited by spark immediately after the emergence of the cool flame, being substantially longer if the mixture is ignited a long time after the cool flame extinguished" (cited after [16]). It is interesting that when the mixture was ignited before the emergence of the cool flame ($t_i < \tau$), the detonation velocity D measured over a distance $L > S$ was 1970 m/s, whereas it was only 1720 m/s when measured after the cool-flame oxidation ($t_i > \tau$) of the mixture (13% lower).

The observed effect of sharp decrease in the predetonation distance (hereafter, the Shchelkin–Sokolik effect) was interpreted by the authors of [10] as arising because the oxidation process significantly changes the reactive-kinetic properties of the mixture. On the one hand, during the cool flame induction period, active products are formed in the mixtures, such as hydroperoxides, which, decomposing in the cool flame, produce new active species and accelerate the oxidation reaction, thereby enhancing the detonatability of the mixture. On the other hand, the abovementioned decrease in the detonation velocity observed when the mixture is ignited immediately after the cool flame extinguished is indicative of a reduction in the heat of combustion of the mixture, since part of it was already released during the cool-flame process (up to 10%); this reduction also manifests itself through decreases in the combustion temperature and laminar flame speed. According to [10], the existence of a minimum in the S curve is associated with a competition between these two factors: at $t_i - \tau \le 0.5$ s, the first one is predominant, whereas the second one prevails at $t_i - \tau > 0.5$ s. In addition, since the oxidation process continues after the extinction of the cool flame, stable products, such as aldehydes and alcohols, appear in the mixtures, a factor that degrades the detonatability of the mixture [16].

Note that the experimental results obtained in [10] were recently confirmed in [17].

3. FORMULATION OF THE PROBLEM

To quantitatively describe the Shchelkin–Sokolik effect, we formulated the following problem. Let a straight tube of length L be filled by a homogeneous n-pentane–oxygen mixture at an initial pressure p_0 and initial temperature T_0. Let the tube be closed at each end and thermally insulated. Given that in the experiments performed in [10], detonation arose in the region between the shock wave and accelerating flame front, we simplified the problem by excluding from consideration both spark ignition and the accelerating flame. Instead, we considered a shock wave of preset initial intensity propagating from one of the ends ($x = 0$) of the closed tube. The shock wave intensity was selected based on the fact that the direct initiation of detonation in stoichiometric fuel–oxygen mixtures can be accomplished by a shock wave capable of creating a compressed-gas temperature of 1100–1200 K. At normal initial conditions, such temperatures are achieved behind shock waves with a Mach number of $M = 3.2$–3.5; at elevated initial temperatures (600–900 K in [10]), it suffices to provide Mach numbers of $M = 1.8$–2.4.

The shock wave was generated by creating a zone ($x \in [0, \delta]$, $\delta \in L$) with increased pressure $p = p_s$ and

density $\rho = \rho_s$. It was assumed that the reacting gas obeys the equation of state of an ideal gas, being, however, viscous and heat conductive. Since the reacting gas consisted of several components, the reactants and reaction products, we took account of the multicomponent molecular diffusion of the mixture component. At the current stage of studies, we ignored turbulent transfer of mass, momentum, and energy. The two-stage autoignition of *n*-pentane–oxygen mixture was described using a semiempirical kinetic mechanism [18] capable of modeling the low- and high-temperature oxidation of *n*-pentane.

Under the above assumptions, the problem was solved using the following system of one-dimensional nonstationary equations of flow.

The mass conservation equation

$$\frac{\partial \rho}{\partial t} + \frac{\partial}{\partial x}(\rho u) = 0. \quad (1)$$

The momentum conservation equation

$$\frac{\partial u}{\partial t} + u\frac{\partial u}{\partial x} = -\frac{1}{\rho}\frac{\partial p}{\partial x} + \mu\frac{\partial^2 u}{\partial x^2}. \quad (2)$$

The species conservation equation

$$\frac{\partial y_i}{\partial t} = -u\frac{\partial y_i}{\partial x} + \frac{\omega_i}{\rho} - \frac{1}{\rho}\frac{\partial}{\partial x}(\rho V_i y_i). \quad (3)$$

The energy conservation equation

$$C_V\frac{\partial T}{\partial t} = -C_V u\frac{\partial T}{\partial x} - \frac{1}{\rho}\sum_i\left(h_i - \frac{R_0 T}{w_i}\right)\omega_i$$
$$-\frac{1}{\rho}\frac{\partial T}{\partial x}\sum_i \rho C_{Pi} V_i y_i - \frac{1}{\rho}R_0 T\sum_i \frac{1}{w_i}\frac{\partial}{\partial x}(\rho V_i y_i) \quad (4)$$
$$+\frac{1}{\rho}\frac{\partial}{\partial x}\left(\lambda\frac{\partial T}{\partial x}\right) - \frac{\partial u}{\partial x}R_0 T\sum_i \frac{y_i}{w_i} + \frac{4}{3}\frac{\mu}{\rho}\left(\frac{\partial u}{\partial x}\right)^2.$$

The equation of state of an ideal gas

$$p = \rho R_0 T\sum_i \frac{y_i}{w_i}. \quad (5)$$

Here, t is the time; x is the longitudinal coordinate; ρ is the density; u is the velocity; p is the pressure; T is the temperature; C_V is the heat capacity of the mixture at constant volume; R_0 is the universal gas constant; h_i, y_i, V_i, w_i, C_{Pi}, and ω_i are the enthalpy, mass concentration, diffusion rate, molecular mass, heat capacity at constant pressure, and overall rate of chemical reactions of the ith component of the mixture, respectively; and μ and λ are the dynamic viscosity and thermal conductivity of the mixture.

Let

$$C = \sum_i \frac{y_i}{w_i},$$

$$a_{ij} = -\frac{y_i}{w_i D_{ij} C}\ (i \neq j),$$

$$a_{ii} = \sum_{i \neq j}\frac{y_i}{w_i D_{ij} C},$$

$$g_i = \frac{\partial y_i}{\partial x} - y_i\frac{\partial C}{\partial x}C$$

(where D_{ij} is the binary diffusion coefficient of the ith component of the jth component), then

$$\sum_j a_{ij} y_j V_j = g_i$$

and

$$\sum_j y_j V_j = 0.$$

The molecular transport coefficients μ, λ, and D_{ij} were calculated by the formula presented in [19].

The system of equations (1)–(5) was supplemented with the following boundary

$$\left.\frac{\partial \rho}{\partial x}\right|_{x=0} = \left.\frac{\partial \rho}{\partial x}\right|_{x=L} = 0, \quad u(0) = u(L) = 0,$$
$$\left.\frac{\partial y_i}{\partial x}\right|_{x=0} = \left.\frac{\partial y_i}{\partial x}\right|_{x=L} = 0, \quad \left.\frac{\partial T}{\partial x}\right|_{x=0} = \left.\frac{\partial T}{\partial x}\right|_{x=L} = 0, \quad (6)$$

and initial conditions:

$$\text{at } t = 0 \text{ and } 0 \le x \le \delta\text{: } u(0,x) = 0,\ \rho(0,x) = \rho_s,$$
$$y_i(0,x) = y_{i0}^*(0,x), \quad T(0,x) = T_0^*;$$
$$\text{at } t = 0 \text{ and } \delta < x \le L\text{: } u(0,x) = 0,\ \rho(0,x) = \rho_0^*, \quad (7)$$
$$y_i(0,x) = y_{i0}^*(0,x), \quad T(0,x) = T_{i0}^*.$$

The initial concentrations y_{i0} of the components were calculated from the specified fuel equivalence ratio Φ. A thermal pretreatment of the explosive mixture may cause a change of the initial values of the variables (as in [10]), a factor that should be taken into account while solving the problem. The initial values of the variables y_{i0}^*, ρ_0^*, and T_0^* were selected with consideration given to this circumstance.

One specific feature of the system of equations (1)–(5) is that the mass conservation equation and momentum conservation equation (at $\mu = 0$) are first-order differential equations, with two boundary conditions being specified for each of ρ and u. To demonstrate the correctness of the problem posed, we extended the distributions of the variables ρ, p, T, and y_i to the segment $[-L, 0]$ in an even manner (for example, $\rho(-x) = \rho(x)$) and the distribution of u, in an odd manner ($u(-x) = -u(x)$). It is easy to see that all equations preserve the evenness–oddness properties. Let us now extend the distributions of the indicated variables in a $2L$-periodic manner. In this formulation, the gov-

erning equations describe the distributions of $2L$-periodic functions, and, therefore, the imposed boundary conditions are satisfied automatically.

To simplify numerical calculations, we introduced new variables:

$$\phi = \frac{P}{\rho}, \quad z_p = \rho\exp\left(\frac{u}{\sqrt{\phi}}\right), \quad z_m = \rho\exp\left(-\frac{u}{\sqrt{\phi}}\right).$$

Then, for the segment $x \in [0, L]$, we can write

$$\frac{\partial z_p}{\partial t} = -(u + \sqrt{\phi})\frac{\partial z_p}{\partial x}$$

$$- z_p\left[u\frac{\partial\phi}{\partial t} + (u^2 + u\sqrt{\phi} + 2\phi)\frac{\partial\phi}{\partial x}\right]/2\phi\sqrt{\phi},$$

$$\frac{\partial z_m}{\partial t} = (u + \sqrt{\phi})\frac{\partial z_m}{\partial x}$$

$$+ z_m\left[u\frac{\partial\phi}{\partial t} + (u^2 - u\sqrt{\phi} + 2\phi)\frac{\partial\phi}{\partial x}\right]/2\phi\sqrt{\phi},$$

where $z_p(0) = z_m(0)$, $z_p(L) = z_m(L)$, and

$$\frac{\partial(z_p + z_m)}{\partial x}\bigg|_{x=0} + \frac{\partial(z_p + z_m)}{\partial x}\bigg|_{x=L} = 0.$$

Let z be a $2L$-periodic function within the segment $[-L, L]$, defined as

$$z(x) = \begin{cases} z_p(x) & \text{at } x \geq 0 \\ z_m(x) & \text{at } x \leq 0. \end{cases}$$

Then,

$$\frac{\partial z}{\partial t} = -(u + \sqrt{\phi})\frac{\partial z}{\partial x} + \frac{4}{3}\frac{\mu}{\rho\sqrt{\phi}}\frac{\partial^2 u}{\partial x^2}z$$

$$- \frac{z}{2\phi\sqrt{\phi}}\left(u\frac{\partial\phi}{\partial t} + (u^2 + u\sqrt{\phi} + 2\phi)\frac{\partial\phi}{\partial x}\right). \quad (8)$$

Note that the boundary conditions for this equation are satisfied automatically. Equation (8) replaces Eqs. (1) and (2) for ρ and u in the original system of equations. These variable are calculated by the formulas

$$\rho(x) = \sqrt{z(x)z(-x)},$$

$$u(x) = \frac{\sqrt{\phi}}{2}\ln\frac{z(x)}{z(-x)}.$$

Introducing the function $a = u + \sqrt{\phi}$ makes it possible to solve Eq. (8) along the curves described by the equation

$$\frac{\partial x}{\partial t} = a(t; x(t)).$$

In this case, Eq. (8) can be presented in a simple form:

$$\frac{\partial z}{\partial t} = zu\frac{d}{dt}\left(\frac{1}{\sqrt{\phi}}\right) + \left(\frac{4}{3}\frac{\mu}{\rho\sqrt{\phi}}\frac{\partial^2 u}{\partial x^2} - 2\frac{\partial}{\partial x}(\sqrt{\phi})\right)z.$$

The problem posed was solved using the finite difference method of first order in time and space. Calculations were performed on an adaptive computational grid, with an automatic adjustment of the time step and the mesh point density in the region of high gradients of the dependent variables.

4. CALCULATION RESULTS

Semiempirical Mechanism of the Oxidation of n-Pentane

A semiempirical kinetic mechanism of the two-stage oxidation of *n*-pentane and the kinetic parameters of the reactions are listed in the table. The mechanism was compiled based on the principle proposed in [18], with switching the value of the limiting reaction at the boundary between high and low temperatures (950 K). The mechanism includes seven reactions. The results of calculations of the autoignition delay time τ_{ign} at various temperatures and pressures within the framework of this mechanism implemented in a standard program demonstrate a close agreement with the available experimental data [20, 21] (Fig. 2). The calculations were performed under assumption that, in the course of the reaction, the pressure remains unchanged.

Kinetic calculations of the oxidation of an *n*-pentane–oxygen stoichiometric mixture with account of heat transfer to the wall under the conditions identical to those employed in [10] showed that, at a certain moment, a cool flame arises (Fig. 3). The heat transfer coefficient was set equal to the value characteristic of a quiescent medium, $\alpha = 2370$ W/m^3. As a cool flame appears at $t \approx 0.15$–0.21 s, the temperature of the mixture increases from the initial value 608 K to its maximum, 930 K (Fig. 3).

Propagation of a Shock Wave through an n-Pentane–Oxygen Mixture

Using the kinetic mechanism presented in the table, we performed a series of numerical simulations of the propagation of a shock wave in a tube filled with an *n*-pentane–oxygen mixture at the following initial parameters: $L = 0.24$ m, $\delta = 0.03$ m, $T_0 = 608$ K, $p_0 = 0.42$ atm, $p_s = 10$ atm, and $\Phi = 1$. To simulate the effect of a thermal pretreatment of the explosive mixture on the initial values of the variables (condition (7)), we used a standard kinetic program: the shock wave was generated in a mixture with a composition y_{i0}^*, density ρ_0^*, and temperature T_0^*; the values of these parameters were determined by performing kinetic calculations within a time interval equal to the ignition delay t_i measured in [10].

The calculated pressure and temperature profiles along the tube at various instants of time for $t_i = 0$, i.e., without thermal pretreatment of the mixture (at $y_{i0}^* = y_{i0}$, $\rho_0^* = \rho_0$, and $T_0^* = T_0$) are displayed in Figs. 4 and

Mechanism of oxidation and combustion of *n*-pentane

No.	Reaction	A_i, mol, l, s	m_i	E_i, kcal/mol	n_i	Note
1	$C_5H_{12} + 5.5O_2 \longrightarrow 5CO + 6H_2O$	3.64×10^{10}	0	27	0	$T < 950$ K
		1.72×10^{12}	0	45	0	$T > 950$ K
2	$H_2 + H_2 + O_2 \longrightarrow 2H_2O$	7.00×10^{13}	0	21	−0.5	
3	$CO + CO + O_2 \longrightarrow 2CO_2$	8.50×10^{12}	0	21	−1.5	
4	$CO + H_2O \longrightarrow CO_2 + H_2$	1.00×10^{12}	0	41.5	−1	
−4	$CO_2 + H_2 \longrightarrow CO + H_2O$	3.10×10^{13}	0	49.1	−1	
5	$H_2O + M \longrightarrow H + OH + M$	2.85×10^{15}	0	120	0	
−5	$H + OH + M \longrightarrow H_2O + M$	3.6×10^{13}	−1	0	0	

Note: The reaction rate constants were presented as $k_i = A_i p^{ni} \exp(-E_i/RT)$. The rate of reaction no. 1 is given by $W_1 = k_1[C_5H_{12}][O_2]$.

5. As can be seen, without thermal pretreatment of the mixture, the pressure profile in the shock wave looks very much as if the shock wave propagated through an inert gas. Nevertheless, the temperature profiles (Fig. 5) are indicative of a heat release due to cool-flame reactions behind the shock wave front: until the wave reaches the right end face, the temperature at its front increases by 70–80 K, but no autoignition occurs. According to the definition of the predetonation distance given in [10], we set $S > L = 0.24$ m.

The calculated pressure and temperature profiles along the tube at various instants of time for $t_i = 0.2$ s, i.e., after thermal pretreatment of the mixture for a time interval within which a cool flame arises (Fig. 3) are shown in Figs. 6 and 7. Kinetic calculations show that, by the time $t_i = 0.2$ s, the cool flame heats the mixture to $T_0^* \approx 900$ K (curve *1* in Fig. 7a), and its composition changes. At $t \approx 0.200119$ s, i.e., $\Delta t \approx 119$ μs after the shock wave began to propagate (curves *5* in Figs. 6 and 7), autoignition occurs behind its front. As a result, two blast waves are rapidly formed in the shock-compressed gas: an overdriven detonation wave, which overtakes the primary shock wave, and a retonation, which propagates in the opposite direction. That the overpressure in the overdriven detonation wave is relatively low (~17–18 atm) can be accounted for by the low density of the mixture ahead of the shock wave front. At $\Delta t > 129$ μs, a self-sustained detonation wave propagates toward the right end face with a mean calculated detonation velocity of ~1990 m/s, a value very close to 1970 m/s measured in [10]. Based on the definition of the predetonation distance suggested in [10], we estimated this quantity as $S \approx 0.122$ m. Thus, comparing the results presented in Figs. 4, 5 and Figs. 6, 7, we concluded that the ther-

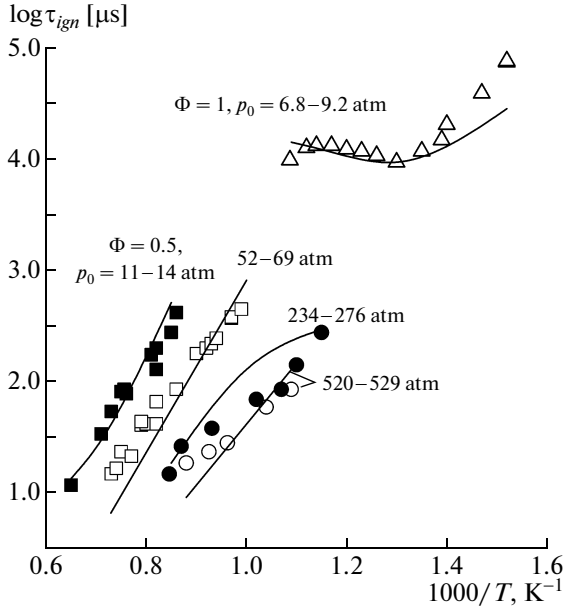

Fig. 2. Calculated (curves) and measured (points) temperature dependences of the autoignition delay time for *n*-pentane at various pressures. The experiments were performed at $\Phi = 1.0$ [21] and 0.5 [22].

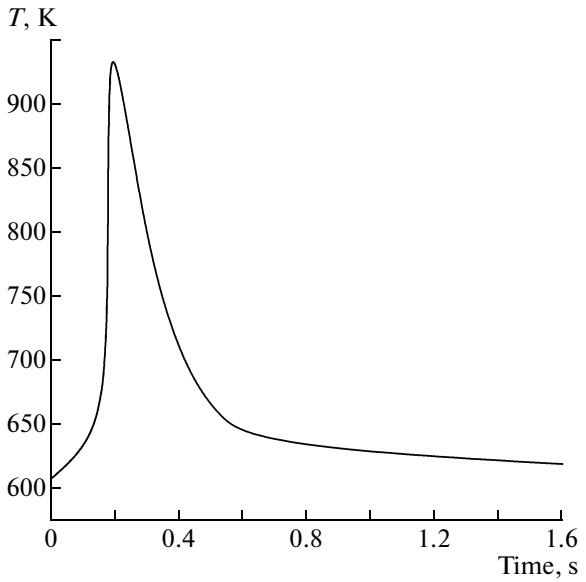

Fig. 3. Temperature time history for the oxidation of a $C_5H_{12} : 8O_2$ (stoichiometric) mixture at $T_0 = 608$ K and $p_0 = 0.42$ atm.

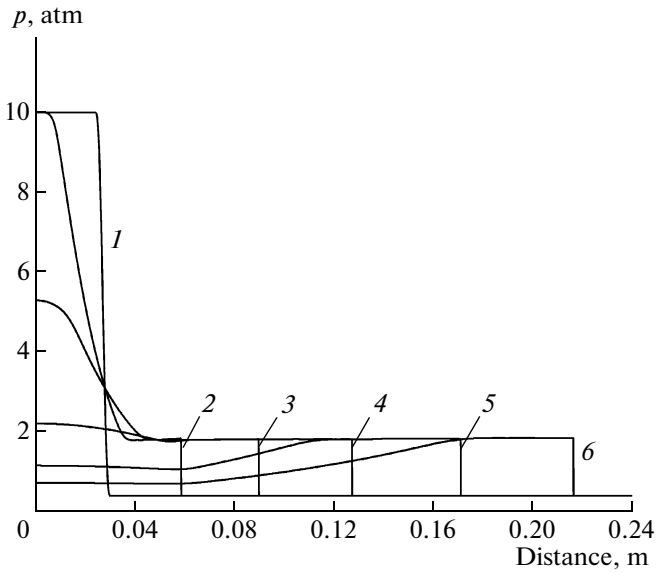

Fig. 4. Calculated pressure profiles in the shock wave in the absence of thermal pretreatment of an *n*-pentane–oxygen stoichiometric mixture ($t_i = 0$) at $T_0 = 608$ K, $p_0 = 0.42$ atm, and various moments of time (in μs): (*1*) 0, (*2*) 43.4, (*3*) 87.2, (*4*) 141, (*5*) 204, and (*6*) 270.

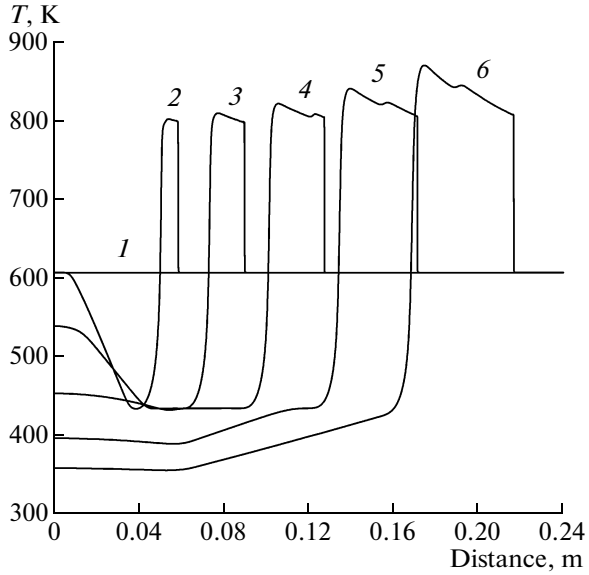

Fig. 5. Calculated temperature profiles in the shock wave in the absence of thermal pretreatment of an *n*-pentane–oxygen stoichiometric mixture ($t_i = 0$) at $T_0 = 608$ K, $p_0 = 0.42$ atm, and various moments of time (in μs): (*1*) 0, (*2*) 43.4, (*3*) 87.2, (*4*) 141, (*5*) 204, and (*6*) 270.

mal pretreatment of the reaction mixture with a cool flame enhances its detonatability.

Detailed Mechanism of n-Pentane Oxidation

To understand how the intermediate species produced by cool-flame oxidation affect the propagation of a shock wave through an *n*-pentane–oxygen mixture, we conducted simulations within the framework of the kinetic mechanism proposed in [22]. This mechanism for describing the gas-phase kinetics of the oxidation and combustion of pentane consists of 387 elementary reversible reactions involving 77 species. Since the experiments in [10] were conducted at a relatively low initial pressure in a tube with a small internal diameter, it is necessary to take into account not only heat transfer to the wall, but also, in the general case, loss of active species on the wall.

Since little is known about the wall reactions involved in the oxidation of hydrocarbons, we limited ourselves to considering two effective diffusion-controlled reactions of decomposition of pentyl hydroperoxide $C_5H_{11}O_2H$ and hydrogen peroxide H_2O_2 with the formation of stable products:

$$C_5H_{11}O_2H \longrightarrow C_5H_{12} + O_2,$$

$$H_2O_2 \longrightarrow H_2O + 0.5O_2.$$

The diffusion rate constant for such reactions is normally given by [23]

$$k = 23.2\frac{D}{d^2},$$

where D is the effective diffusion coefficient and d is the reactor diameter.

The calculated time dependences of the temperature and hydrogen peroxide concentration at two values of the rate constant for the loss of the peroxides on the wall, $k = 0$ and $k = 9.55$ s^{-1}, under the experimental conditions used in [10] are displayed in Fig. 8. The calculations were performed using a standard chemical kinetics program on the assumption that the process proceeds at constant pressure. The cool flame manifested itself as a series of multiple light flashes, so-called multiple cool flame (Fig. 8a); Fig. 8b shows the same results with a better time resolution. The cool flame arises due to the accumulation of pentyl hydroperoxide accompanied by the formation of hydroxyls, which substantially speed up the oxidation process and temperature rise. After the first flash, only a low concentration of pentyl hydroperoxide remains, whereas the concentration of hydrogen peroxide increases but eventually decreases due to its loss on the walls.

Unfortunately, the detailed kinetic mechanism is too large to be used in calculations of the propagation of a shock wave in a tube filled with a pentane–oxygen mixture; instead, we performed a series of kinetic calculations.

First, at the temperatures and pressures identical to those used in the experiments performed in [10], we calculated the evolution of the composition and temperature with time. This yielded information about the effect of the duration of thermal pretreatment (spark ignition delay t_i) on the temperature and composition of the mixture. Then, we performed a series of calcu-

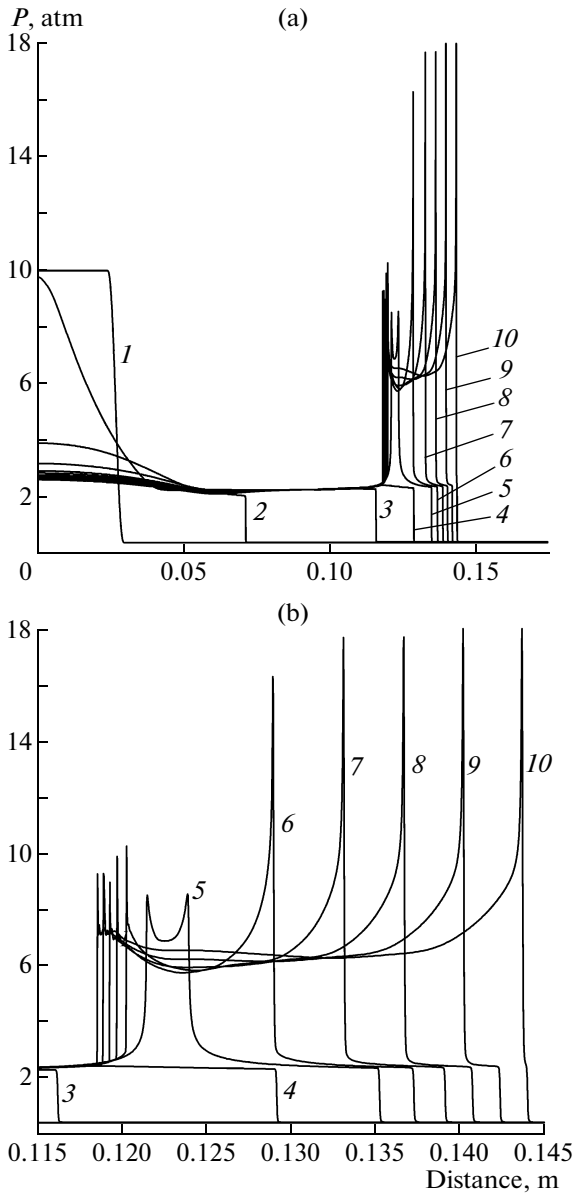

Fig. 6. Calculated pressure profiles in the shock wave upon thermal pretreatment (for t_i = 0.2 s) of an *n*-pentane–oxygen stoichiometric mixture at T_0 = 608 K, p_0 = 0.42 atm, and various moments of time (in s): (*1*) 0.2, (*2*) 0.200050, (*3*) 0.200098, (*4*) 0.200112, (*5*) 0.200119, (*6*) 0.200121, (*7*) 0.200123, (*8*) 0.2001247, (*9*) 0.2001261, (*10*) 0.2001281. (a) The overall picture and (b) detonation formation region.

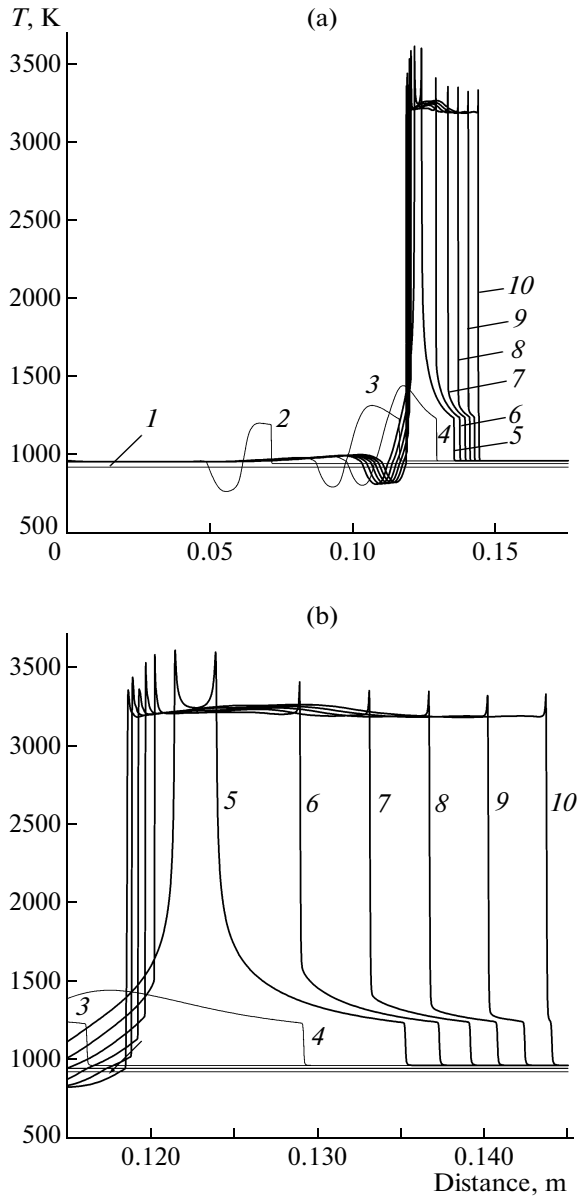

Fig. 7. Calculated temperature profiles in the shock wave upon thermal pretreatment (for t_i = 0.2 s) of an *n*-pentane–oxygen stoichiometric mixture at T_0 = 608 K, p_0 = 0.42 atm, and various moments of time (in s): (*1*) 0.2, (*2*) 0.200050, (*3*) 0.200098, (*4*) 0.200112, (*5*) 0.200119, (*6*) 0.200121, (*7*) 0.200123, (*8*) 0.2001247, (*9*) 0.2001261, (*10*) 0.2001281. (a) The overall picture and (b) detonation formation region.

lations of the characteristics of autoignition of thermally pretreated mixture behind shock waves with Mach number from 1.8 to 2.4 (see above).

Figure 9 shows the calculated temperature at the shock wave front T_{sw} and the delay time of autoignition τ_{ign} behind the shock wave as a function of the duration of thermal pretreatment t_i. The autoignition delay time was calculated at two values of the rate of loss of the hydroperoxides on the wall: $k = 0$ and $k = 9.55\ s^{-1}$. The shock wave velocity was set equal to D_{sw} = 1025 m/s ($M \approx 2.3$ at T_0 = 608 K). Under these conditions, the temperature at the shock wave front T_{sw} is high enough (1100–1200 K) to directly initiate detonation in mixtures of hydrocarbons with oxygen (Fig. 9). The temperature T_{sw} and autoignition delay time τ_{ign} are nonmonotonic functions of t_i. The temperature T_{sw} achieves its maximum value as the cool flame temperature does. At $k = 0$, the minimum in the $\tau_{ign}(t_i)$ curve

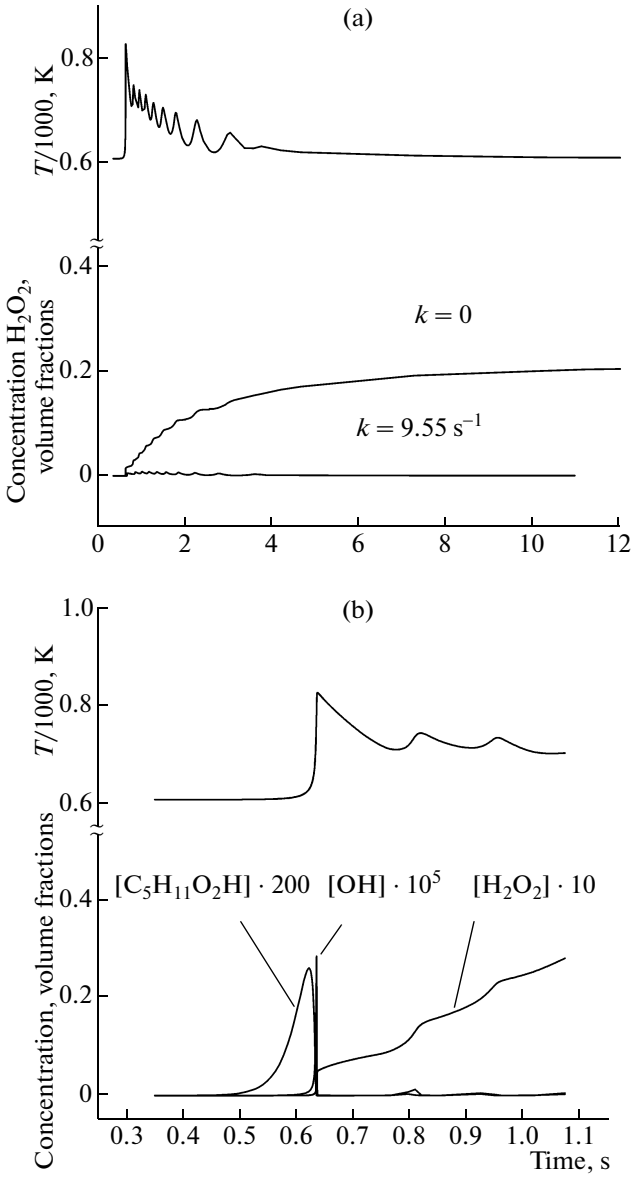

Fig. 8 Calculated time histories of (a) the temperature and hydrogen peroxide concentration at $k = 0$ and $k = 9.55\ s^{-1}$ and (b) the temperature, pentyl hydroperoxide concentration, and hydroxyl concentration at $k = 0$ for a *n*-pentane–oxygen stoichiometric mixture at $T_0 = 608$ K and $p_0 = 0.42$ atm.

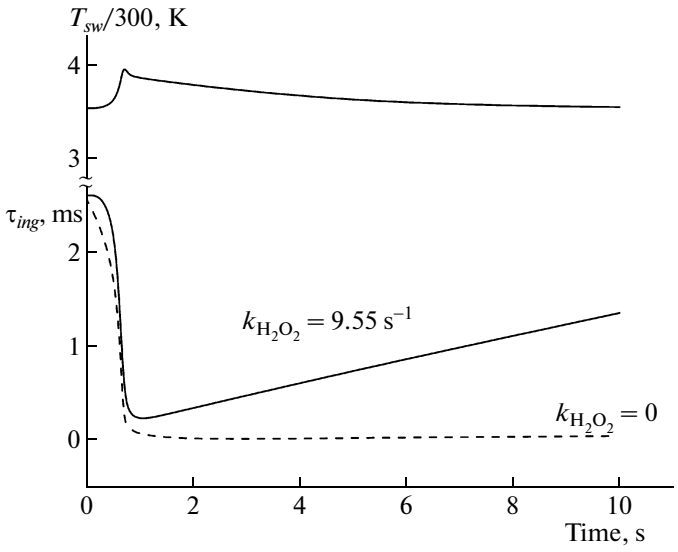

Fig. 9. Calculated dependence of the temperature at the shock wave front T_{sw} and the autoignition delay time for a *n*-pentane–oxygen stoichiometric mixture on the duration of thermal pretreatment of the mixture t_i at $k = 0$ and $k = 9.55\ s^{-1}$ and the initial conditions $T_0 = 608$ K and $p_0 = 0.42$.

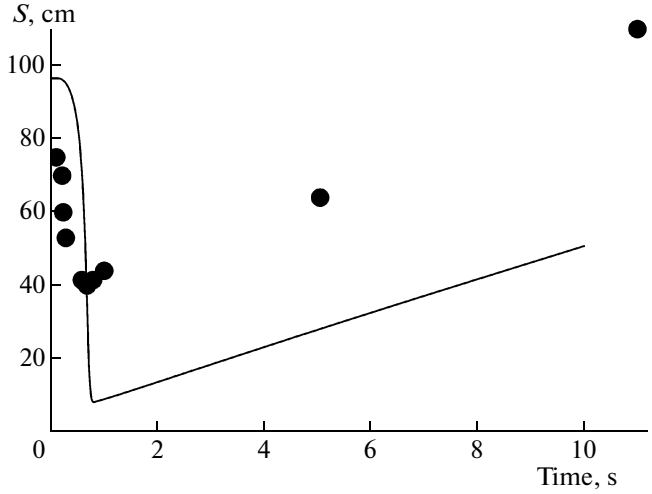

Fig. 10. Comparison of the calculated (curve) and measured (points from [10]) dependences of the predetonation distance S on the duration of thermal pretreatment t_i of a *n*-pentane–oxygen stoichiometric mixture at $T_0 = 608$ K and $p_0 = 0.42$.

is very weak, whereas, at $k = 9.55\ s^{-1}$, it is well pronounced and also is achieved at a time close to the moment the cool flame appears.

According to the definition of the predetonation distance S introduced in [10], the location where detonation arises corresponds to the location at which the mixture autoignites behind the shock wave. To derivative the function $S(t_i)$ from the $\tau_{ign}(t_i)$ dependence (as in Fig. 9), one can use the formula

$$S = D_{sw}\rho_0\frac{\tau_{ign}}{\rho_{sw}},$$

where ρ_{sw} is the density of the mixture behind the shock wave front. Figure 10 compares the measured [10] (points) and calculated (curve) $S(t_i)$ dependences. The calculations were performed at $k = 9.55\ s^{-1}$. As can be seen, the calculation results are in close agreement with the experimental data from [10], despite the fact that the calculated $S(t_i)$ dependence was obtained without account of the distance over which the shock wave forms and achieves the velocity D_{sw}. Recall that, in experiment [10], detonation was not initiated by a shock wave, but arose due to deflagration-to-detonation transition. Importantly, the minimum value of S

in experiments and in calculations is achieved at close values of t_i.

The calculations results led us to an interesting conclusion: if only heat transfer to the wall is taken into account, without regard for the loss of species on the wall ($k = 0$), the calculated $S(t_i)$ dependence has no pronounced minimum, which, however, is observed in experiment (Fig. 1). This means that wall reactions play an important role in small-diameter tubes at low pressures, as in experiments performed in [10]. For large-diameter tubes and high pressures, the importance of wall reactions should decline, leading to the disappearance of the minimum in the $S(t_i)$ dependence; however, new experiments are needed to confirm this conclusion.

CONCLUSIONS

In the present work, we tried to provide a quantitative theoretical explanation of the Shchelkin–Sokolik effect [10], i.e., the dependence of the predetonation distance on the duration of thermal pretreatment of the explosive mixture before ignition with an external source. Gasdynamic calculations of the direct initiation of detonation in an *n*-pentane–oxygen mixture with the use of a simplified two-stage mechanism of *n*-pentane oxidation demonstrated that a thermal pretreatment of the mixture really results in a shortening of the predetonation distance. Kinetic calculations of the autoignition of the mixture behind a shock wave based on a detailed kinetic mechanism of *n*-pentane oxidation showed that the shortest autoignition delay time (and the smallest predetonation distance) is achieved when a cool flame arises by the moment of arrival of the shock wave. The calculated and measured dependences of the predetonation distance on the duration of thermal pretreatment of the mixture were demonstrated to be in close agreement. It was revealed that wall reactions play an important role at the experimental conditions used in [10].

ACKNOWLEDGMENTS

This work was conducted under the state contract "Development of Methods for Numerical Simulations of Unsteady Combustion and Detonation of Gases and Sprays in Complex-Geometry Channels and Semiconfined Spaces as Applied to Pulsed Detonation Engines" (no. P502) and the state contract "Development of the Process of Pulsed Detonation Combustion of Natural Gas for Enhancement of the Efficiency of Powder Installations" (no. 02.516.12.6026) and was supported by the Russian Foundation for Basic Research, project no. 08-08-00068.

REFERENCES

1. S. M. Frolov, *Pulse Detonation Engines* (Torus Press, Moscow, 2006) [in Russian].
2. S. M. Frolov, Ross. Khim. Zh. **52** (6), 48 (2008).
3. P. Laffitte, Ann. Phys. (N.Y.) **4**, 587 (1925).
4. K. I. Shchelkin, Zh. Eksp. Teor. Fiz. **10**, 823 (1940).
5. S. M. Frolov, I. V. Semenov, P. V. Komissarov, P. S. Utkin, and V. V. Markov, Dokl. Akad. Nauk **415**, 509 (2007).
6. N. N. Smirnov and A. P. Boichenko, Fiz. Goreniya Vzryva, No. 2, 121 (1986).
7. S. M. Frolov, Khim. Fiz. **27** (6), 31 (2008) [Russ. J. Phys. Chem. B **27**, 442 (2008)].
8. C. M. Brophy, J. O. Sinibaldi, F. Wang, et al., AIAA Pap. No. 2004-0834 (2004).
9. S. A. Bozhenkov, S. M. Starikovskaia, and A. Yu. Starikovskii, in *Confined Detonations and Pulse Detonation Engines*, Ed. by G. D. Roy, S. M. Frolov, R. J. Santoro, and S. A. Tsyganov (Torus Press, Moscow, 2002), p. 259.
10. K. I. Shchelkin and A. S. Sokolik, Zh. Fiz. Khim. **10**, 484 (1937).
11. A. J. Higgins, P. Pinard, A. C. Yoshinaka, and J. H. S. Lee, in *Detonation and High-Speed Deflagration*, Ed. by G. D. Roy, S. M. Frolov, D. Netzer, and A. A. Borisov (Torus Press, Moscow, 2001), p. 45.
12. S. M. Frolov, V. S. Aksenov, and V. Ya. Basevich, Dokl. Akad. Nauk **410**, 55 (2006).
13. X. Rocourt, P. Gillard, I. Sochet, D. Piton, and A. Prigent, Shock Waves **16**, 233 (2007).
14. A. M. Starik and N. S. Titova, Khim. Fiz. **20** (5), 17 (2001).
15. G. D. Roy, S. M. Frolov, A. A. Borisov, and D. W. Netzer, Progr. Energy Combust. Sci. **30**, 545 (2004).
16. A. S. Sokolik, *Autoignition, Flame and Detonation in Gases* (Akad. Nauk SSSR, Moscow, 1960; Israel Program for Sci. Translat., Jerusalem, 1963).
17. M. P. Romano, M. I. Radulescu, A. J. Higgins, and J. H. S. Lee, Combust. Flame **132**, 387 (2003).
18. V. Ya. Basevich and S. M. Frolov, Khim. Fiz. **25** (6), 54 (2006).
19. B. V. Lidskii, M. G. Neigauz, V. Ya. Basevich, and S. M. Frolov, Khim. Fiz. **22** (3), 51 (2003).
20. M. Ribaucour, R. Minetti, and L. R. Sochet, Proc. Combust. Inst. **27**, 345 (1998).
21. V. P. Zhukov, V. A. Sechenov, and A. Y. Starikovskii, Combust. Flame **140**, 196 (2005).
22. V. Ya. Basevich, A. A. Belyaev, and S. M. Frolov, Khim. Fiz. **28** (8), 59 (2009) [Russ. J. Phys. Chem. B **28**, 629 (2009)].
23. V. N. Kondrat'ev and E. E. Nikitin, *Kinetics and Mechanism of Gasophase Reactions* (Nauka, Moscow, 1974) [in Russian].